

# Toroidal asymmetry of 2-D divertor heat flux profiles during the ELM and 3-D field application in NSTX

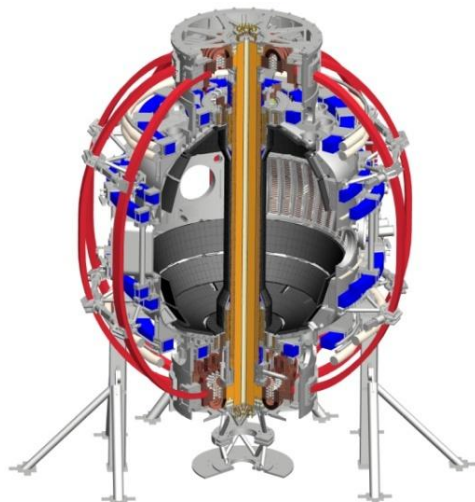
Coll of Wm & Mary  
 Columbia U  
 CompX  
 General Atomics  
 FIU  
 INL  
 Johns Hopkins U  
 LANL  
 LLNL  
 Lodestar  
 MIT  
 Lehigh U  
 Nova Photonics  
 Old Dominion  
 ORNL  
 PPPL  
 Princeton U  
 Purdue U  
 SNL  
 Think Tank, Inc.  
 UC Davis  
 UC Irvine  
 UCLA  
 UCSD  
 U Colorado  
 U Illinois  
 U Maryland  
 U Rochester  
 U Tennessee  
 U Tulsa  
 U Washington  
 U Wisconsin  
 X Science LLC

**J-W. Ahn<sup>1</sup>**


K.F. Gan<sup>2</sup>, F. Scotti<sup>3</sup>, R. Maingi<sup>1</sup>, J.M. Canik<sup>1</sup>, T.K. Gray<sup>1</sup>, J.D. Lore<sup>1</sup>, A.G. McLean<sup>4</sup>, A.L. Roquemore<sup>3</sup>, V.A. Soukhanovskii<sup>4</sup>  
 and the NSTX Research Team

<sup>1</sup>ORNL, <sup>2</sup>ASIPP, <sup>3</sup>PPPL, <sup>4</sup>LLNL

**IAEA Fusion Energy Conference**  
**San Diego, USA**  
**Oct 8 – 13, 2012**

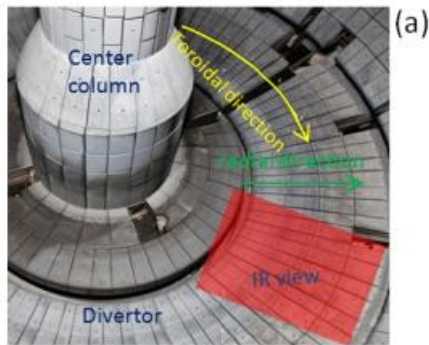


Culham Sci Ctr  
 York U  
 Chubu U  
 Fukui U  
 Hiroshima U  
 Hyogo U  
 Kyoto U  
 Kyushu U  
 Kyushu Tokai U  
 NIFS  
 Niigata U  
 U Tokyo  
 JAEA  
 Inst for Nucl Res, Kiev  
 Ioffe Inst  
 TRINITY  
 Chonbuk Natl U  
 NFRI  
 KAIST  
 POSTECH  
 Seoul Natl U  
 ASIPP  
 CIEMAT  
 FOM Inst DIFFER  
 ENEA, Frascati  
 CEA, Cadarache  
 IPP, Jülich  
 IPP, Garching  
 ASCR, Czech Rep

# Motivation

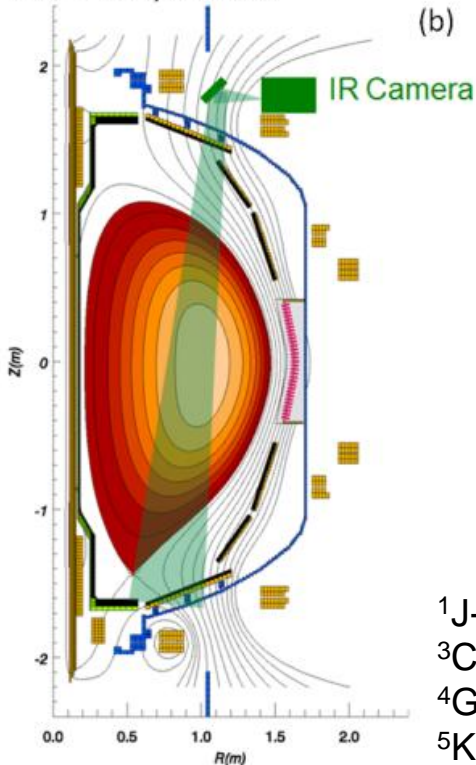
- **Toroidally asymmetric heat flux deposition** is often observed in various physical phenomena, e.g. **ELMs, MHD events, application of 3-D magnetic perturbations, etc**
  - can be harmful to the maintenance of divertor tiles as the design is usually based on the assumption of 2-D axisymmetry
- 1-D heat flux profiles in the radial direction at one toroidal location have been widely used in the divertor heat flux study → **A full 2-D profile is necessary to study toroidally asymmetric heat deposition**
- Conventional heat conduction codes are only able to produce 1-D radial heat flux profiles → need to develop **a novel methodology for 2-D heat flux profiles**

# IR camera diagnostics for heat flux measurement



(a)

Shot= 125059, time= 300



(b)

- Divertor surface temperature is monitored by fast IR camera
- Single band (8-12  $\mu\text{m}$ ) fast IR camera in 2009<sup>1</sup>
  - Spatial resolution: 1.7 mm
  - Temporal resolution: 1.6 – 6.3 kHz
- Dual band (4-6 $\mu\text{m}$  and 7-10  $\mu\text{m}$ ) IR adapter in 2010<sup>2</sup>
  - For lithiated PFC surface, 1.6kHz frame speed
- Heat flux calculation from the measured surface temperature
  - 1-D radial heat flux profile from THEODOR<sup>3</sup>
  - 2-D ( $r, \Phi$ ) heat flux profile from TACO<sup>4</sup>, improved to incorporate thin surface layer effect<sup>5</sup>

<sup>1</sup>J-W. Ahn, RSI 81 (2010), 023501,

<sup>2</sup>A.G. McLean, RSI 83 (2012), 053706

<sup>3</sup>Collaboration with IPP Garching, A. Hermann

<sup>4</sup>G. Castle, COMPASS Note 97.16, UKAEA Fusion (1997)

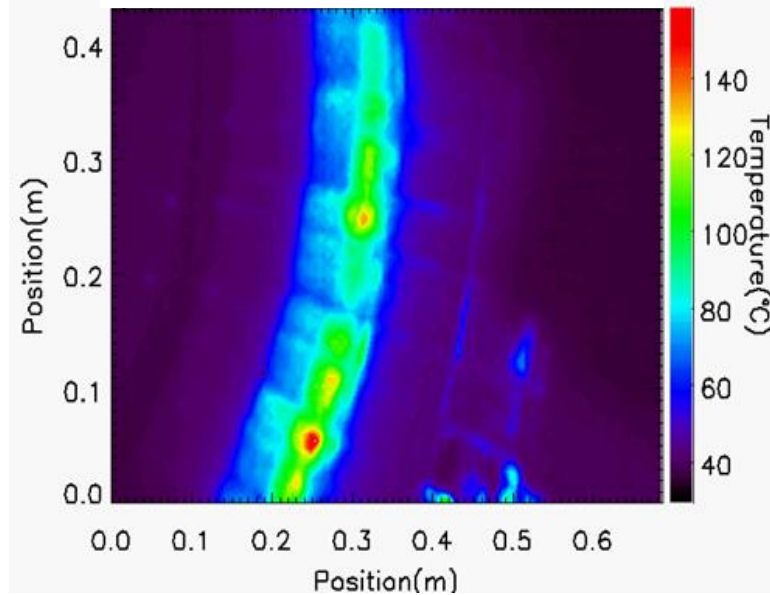
<sup>5</sup>K.F. Gan, submitted to RSI (2012)

# TACO calculates 2-D heat flux distribution at divertor surface

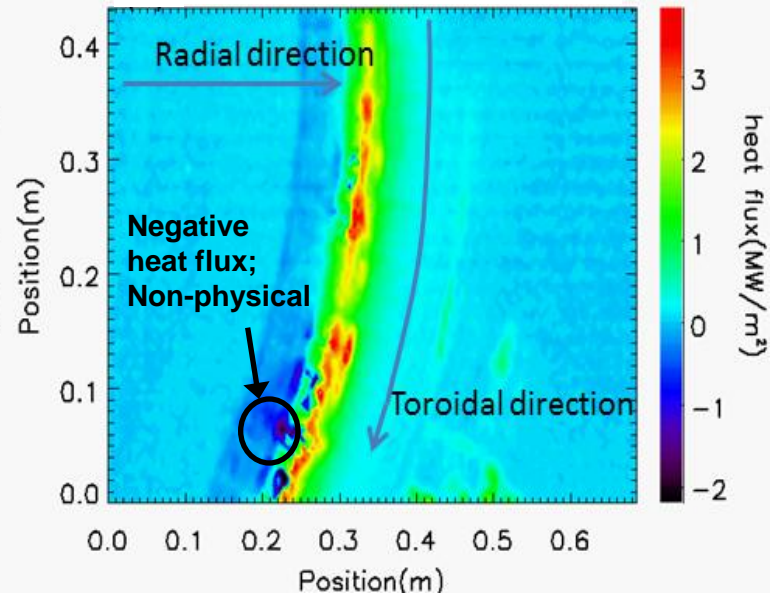
$$Q_{xy}(t_j) = \frac{k\delta}{2\chi\Delta\tau} \frac{(T_{xy}(t_j) - T_{xy}(t_0))}{C_o} - \sum_{\ell=1}^{j-1} Q_{xy}(t_{j-\ell}) \frac{C_l}{C_0}$$

Surface heat flux

**Measured surface temperature**



**Calculated 2-D heat flux**



K.F. Gan, submitted to RSI (2012)

- 2-D heat flux data in (x,y) plane are obtained from TACO
- Toroidally non-axisymmetric 2-D heat flux data are particularly important during the ELMs and 3-D fields application



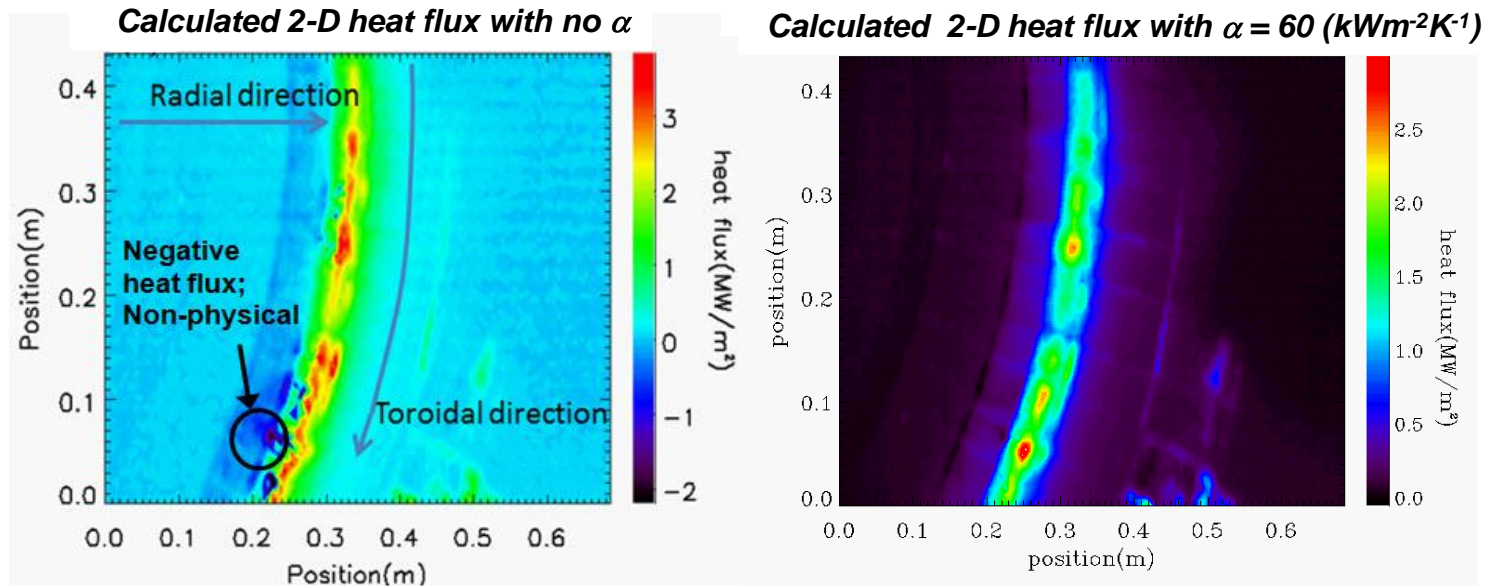
# Implementation of heat transmission coefficient in TACO alleviates negative heat flux problem

$$\alpha = k_{layer} / d \quad \longrightarrow \quad T_{surface} = T_{measured} - \frac{q_s}{\alpha}$$

$\alpha$ : Heat transmission coefficient<sup>1</sup>  
 $k_{layer}$ : surface layer thermal conductivity,  
 $d$ : surface layer thickness

$$Q_{xy}(t_j) = \left( \frac{T_{xy}(t_j) - T_{xy}(t_0)}{C_o} - \sum_{\ell=1}^{j-1} Q_{xy}(t_{j-\ell}) \frac{C_\ell}{C_0} \right) / \left( 1 + \frac{k\delta}{2\chi\Delta\tau C_0\alpha} \right)$$

Surface heat flux with  $\alpha$  incorporated in heat conduction equation



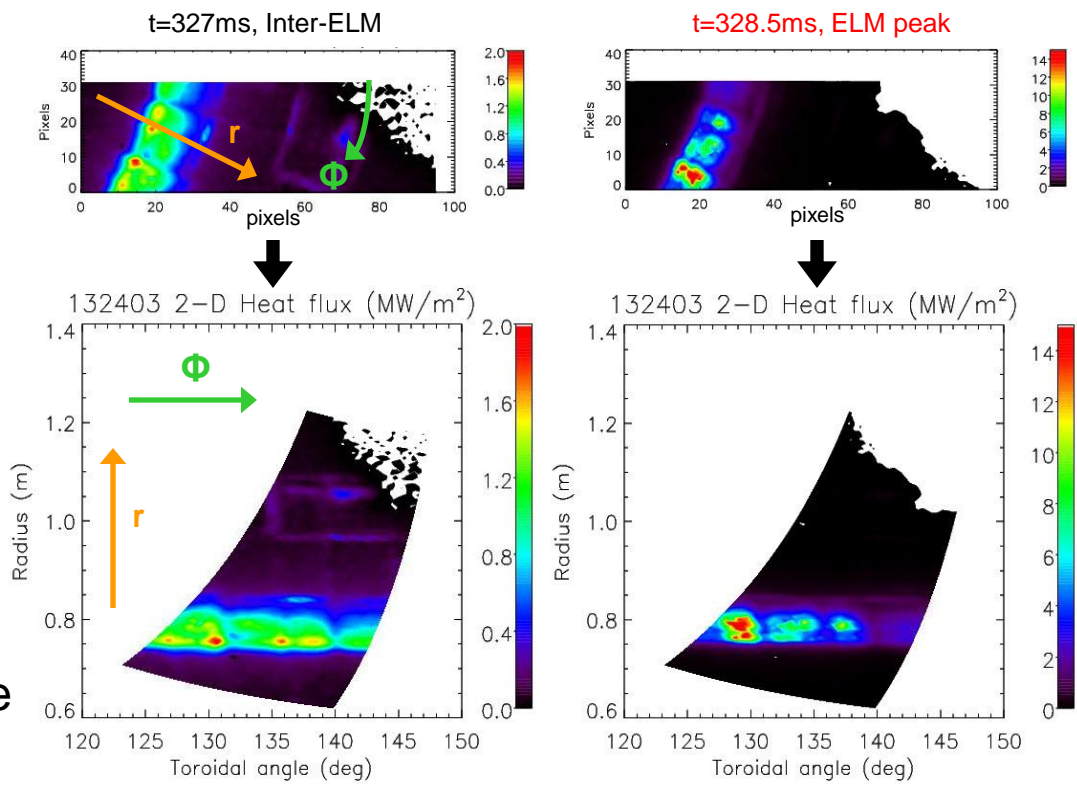
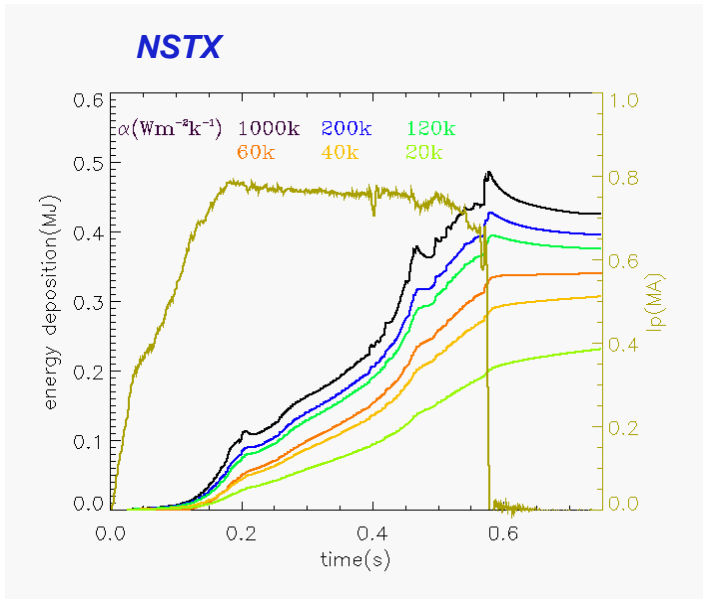
- With  $\alpha$  implemented in the heat conduction equation, negative heat flux problem is alleviated<sup>1,2</sup>. This also lowers the computed peak heat flux

<sup>1</sup> A. Herrmann, PPCF (1995)

International collaboration on THEODOR with IPP-Garching

<sup>2</sup> K.F. Gan, submitted to RSI (2012)

# The calculated 2-D heat flux profiles are re-mapped to $(r, \Phi)$ plane with the choice of $\alpha$ value from the energy conservation



- The  $\alpha$  value makes a large influence on the heat flux calculation, and different values lead to very different results
- In NSTX, an  $\alpha$  value is chosen such that the deposited energy remains constant after the discharge

- The calculated 2-D heat flux profile in  $(x, y)$  plane is re-mapped to the  $(r, \Phi)$  plane.   
 → useful in the study of non-axisymmetric heat flux deposition

# Degree of Asymmetry (DoA) is defined to quantify asymmetric heat deposition onto divertor

$$DoA(q_{peak}) = \sigma_{q_{peak}} / \bar{q}_{peak,2D}$$

$$\bar{q}_{peak,2D} = \sum(q_{peak}) / N$$

$$DoA(\lambda_q) = \sigma_{\lambda_q} / \bar{\lambda}_{q,2D}$$

$$\bar{\lambda}_{q,2D} = \sum(\lambda_q) / N$$

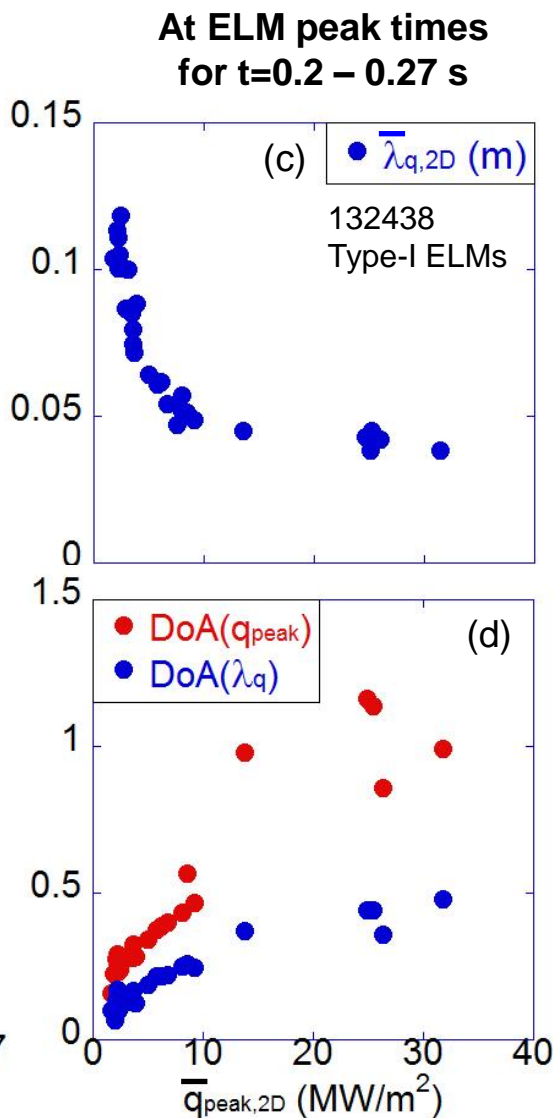
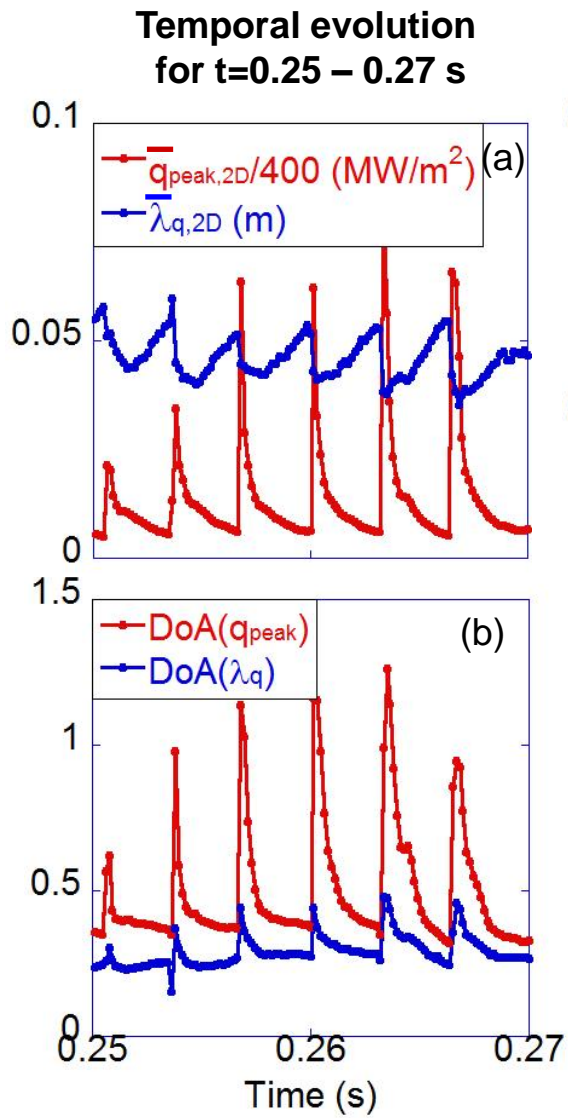
- Define **DoA (Degree of Asymmetry)** for peak heat flux ( $q_{peak}$ ) and heat flux width ( $\lambda_q$ )

- $q_{peak}$  and  $\lambda_q$  is obtained for each radial array of data
- $\sigma_{peak}$  and  $\sigma_{\lambda_q}$  are the standard deviation of  $q_{peak}$  and  $\lambda_q$  over the data in the toroidal direction
- $\sigma_{peak}$  and  $\sigma_{\lambda_q}$  are normalized to the 2-D mean values of  $q_{peak}$  and  $\lambda_q$

- Define mean value of  $q_{peak}$  and  $\lambda_q$ , each to represent the 2-D plane

- N is the total number of toroidal arrays
- $\bar{q}_{peak,2D}$  and  $\bar{\lambda}_{q,2D}$  are the mean values of  $q_{peak}$  and  $\lambda_q$  along the toroidal direction. This represents the whole 2D plane viewed by the IR camera at each time slice

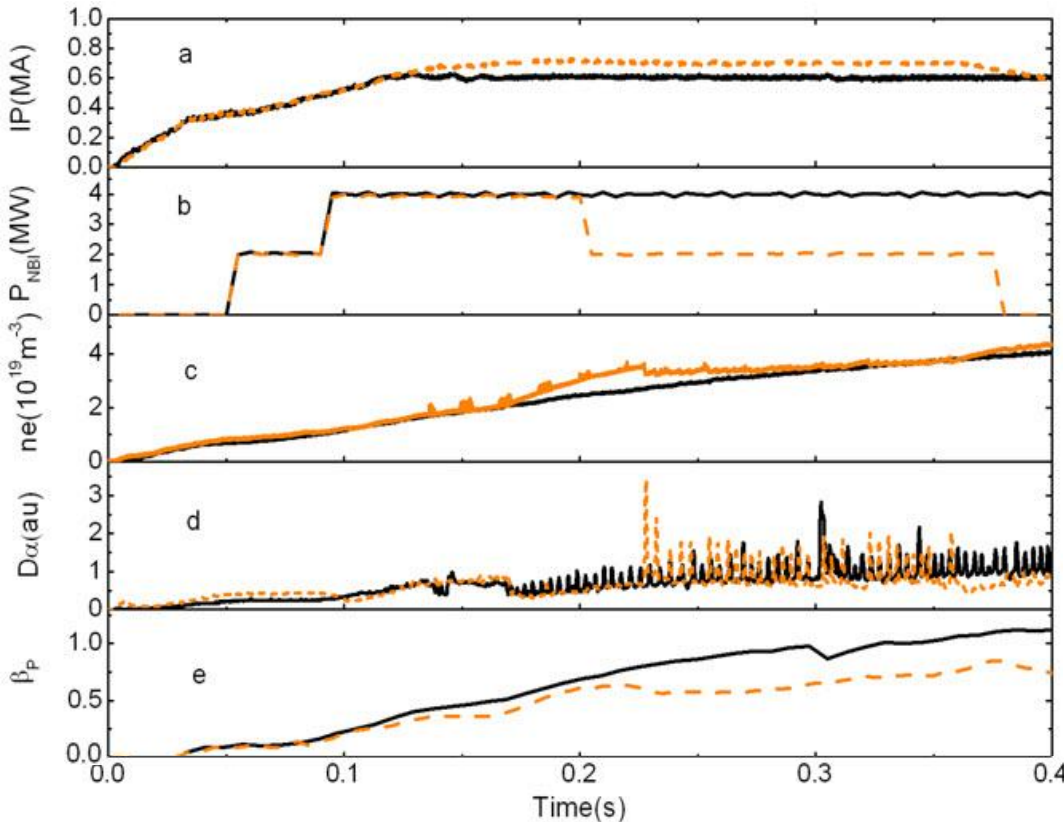
# Degree of Asymmetries increase with rising peak heat flux for ELMs – type-I ELMs



- The 2-D mean value of heat flux width drops during the ELM rise time → **inverse relation between  $\lambda_q$  and  $q_{\text{peak}}$** , contrary to some observations in other tokamaks
- Toroidal asymmetries (DoA) **increase** during the ELM for both  $\lambda_q$  and  $q_{\text{peak}}$
- DoA( $q_{\text{peak}}$ ) is always higher than DoA( $\lambda_q$ ) by a factor 2-3. Both DoAs increase with increasing  $q_{\text{peak}}$



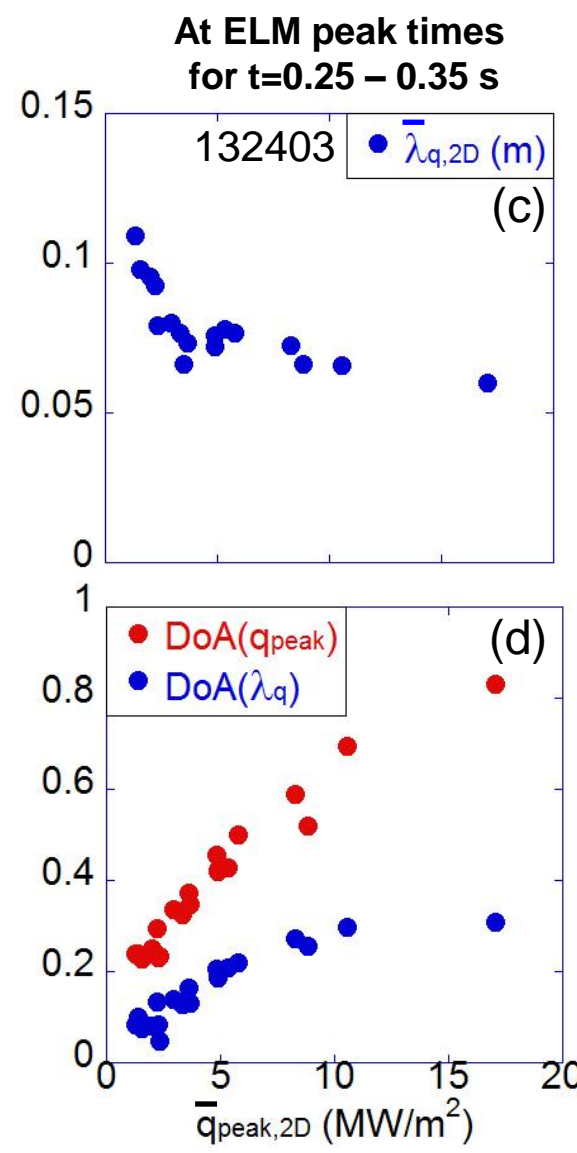
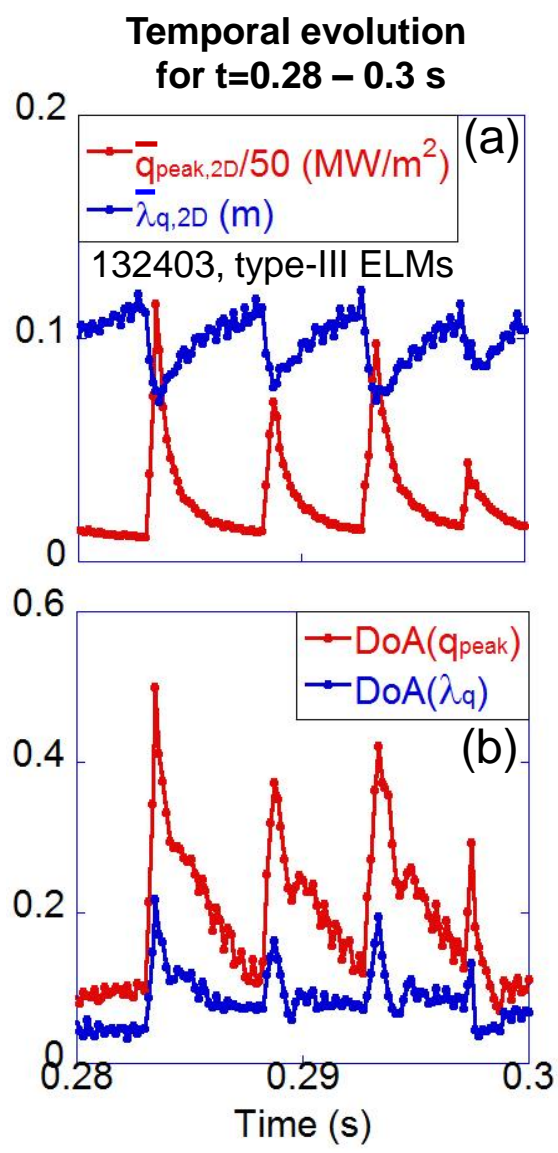
# Distinction between type-III ELMs – high and low $\beta_p$



<sup>1</sup>K.F. Gan, submitted to NF (2012)

- 132401  
 $I_p=600\text{kA}$ ,  $P_{\text{NBI}}=4\text{MW}$   $\rightarrow$  High  $\beta_p$
- 132460  
 $I_p=700\text{kA}$ ,  $P_{\text{NBI}}=2\text{MW}$   $\rightarrow$  Low  $\beta_p$
- Inverse relation between  $q_{\text{peak}}$  and  $\lambda_q$  was revealed for type-III ELMs with high  $\beta_p$ , but the opposite relation is observed for low  $\beta_p$  type-III ELMs<sup>1</sup>
- The poloidal beta ( $\beta_p$ ) has been chosen as a global parameter to represent the pedestal performance  
 $\rightarrow$  Other variables such as pedestal  $T_e$ ,  $n_e$  and the pedestal  $v_e^*$  might better represent the pedestal  
 $\rightarrow$  Work in progress

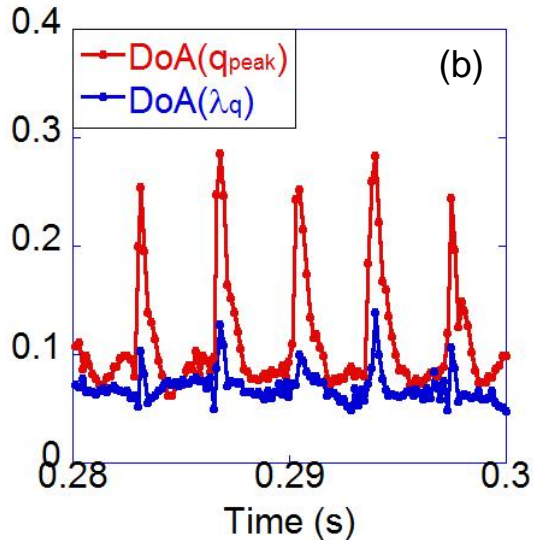
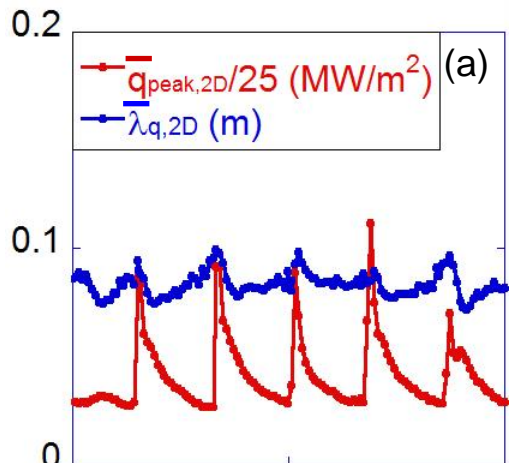
# Degree of Asymmetries increase with rising peak heat flux for ELMs – type-III ELMs with high $\beta_p$



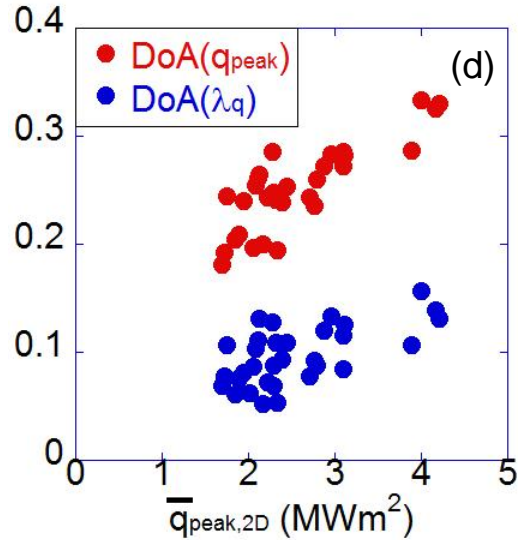
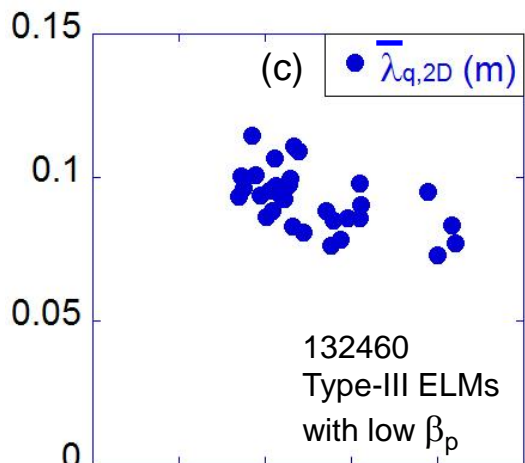
- Similar behaviors to type-I ELMs are observed
  - $\bar{\lambda}_{q,2D} \downarrow$  during the ELM
  - Inverse relation b.t.w.  $\bar{\lambda}_{q,2D}$  and  $\bar{q}_{peak,2D}$  at ELM peak times
- Toroidal asymmetries (DoA) increase again during the ELM
- Both DoAs increase with increasing  $q_{peak}$  but the rate of increase seems to saturate at higher  $q_{peak}$

# $\lambda_q$ during the ELM increases but still decreases with increasing $q_{\text{peak}}$ at ELM peak times – type-III ELMs with low $\beta_p$

Temporal evolution for  $t=0.28 - 0.3$  s



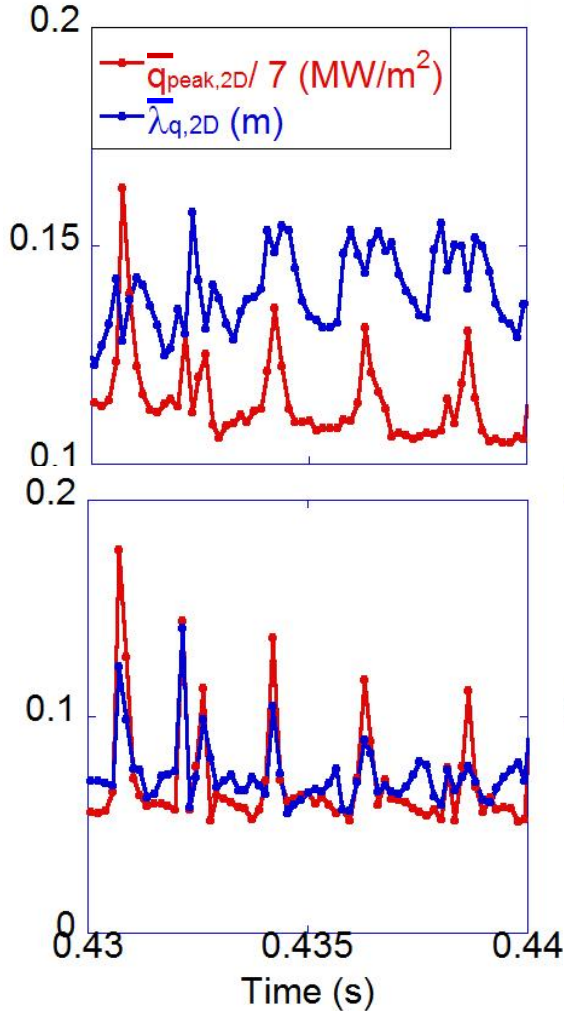
At ELM peak times for  $t=0.24 - 0.35$  s



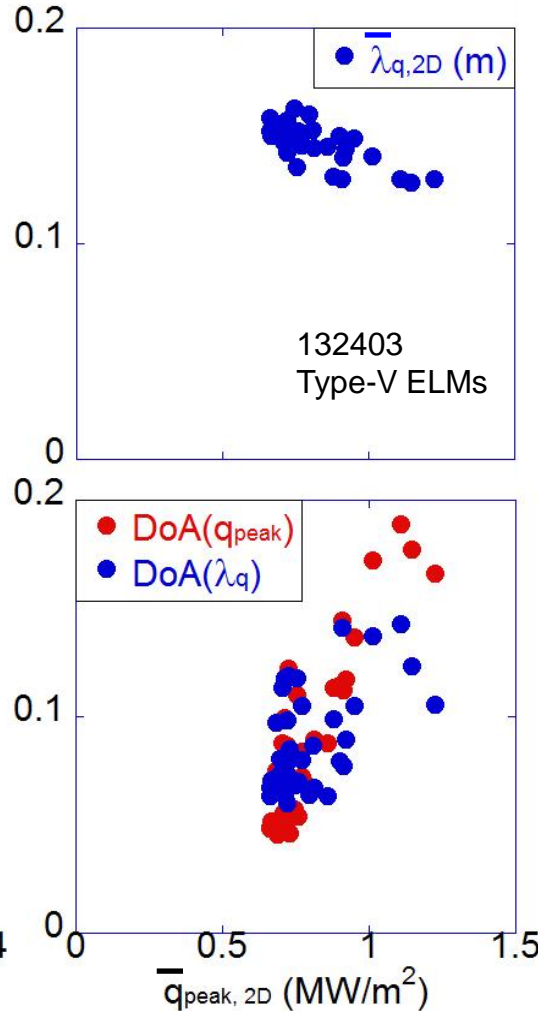
- The 2-D mean value of heat flux width increases during the ELM rise time  $\rightarrow$  the opposite trend to type-III ELMs with high  $\beta_p$
- However, heat flux width at ELM peak times still decreases with increasing peak heat flux
- Similar temporal behavior of the two DoAs; increase during the ELM for both  $\lambda_q$  and  $q_{\text{peak}}$
- DoA( $q_{\text{peak}}$ ) is also higher than DoA( $\lambda_q$ ). The absolute value of both DoA is much smaller than the high  $\beta_p$  case

# $\lambda_q$ during the ELM increases and the Degree of Asymmetry for $q_{\text{peak}}$ and $\lambda_q$ is similar – type-V ELMs

Temporal evolution for  $t=0.43 - 0.44$  s



At ELM peak times for  $t=0.42 - 0.48$  s

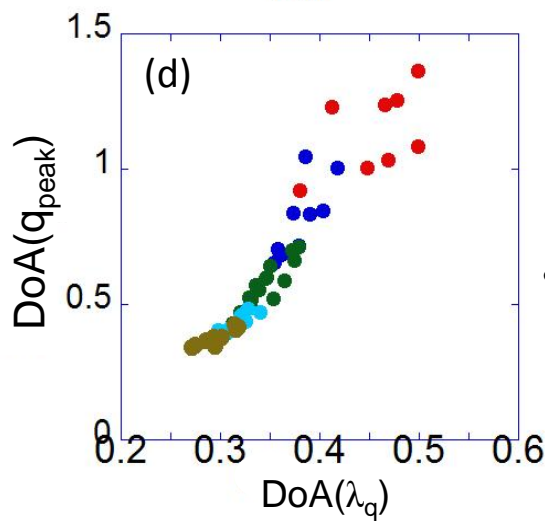
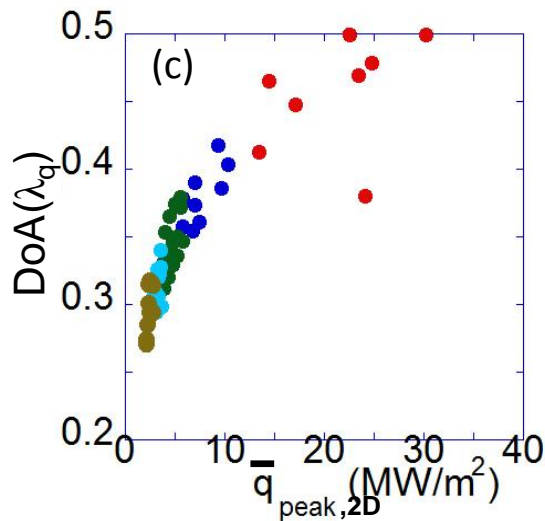
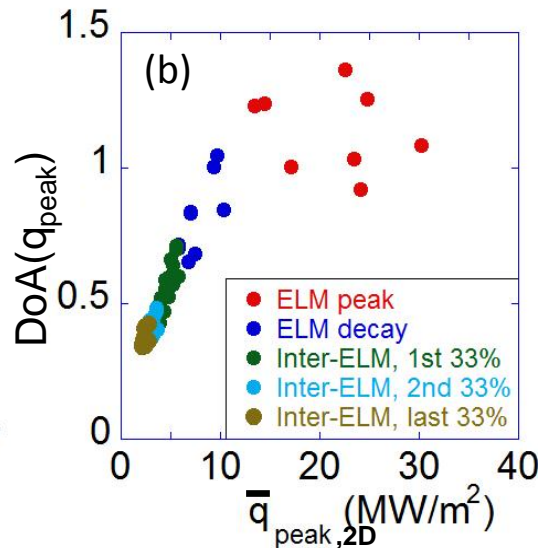
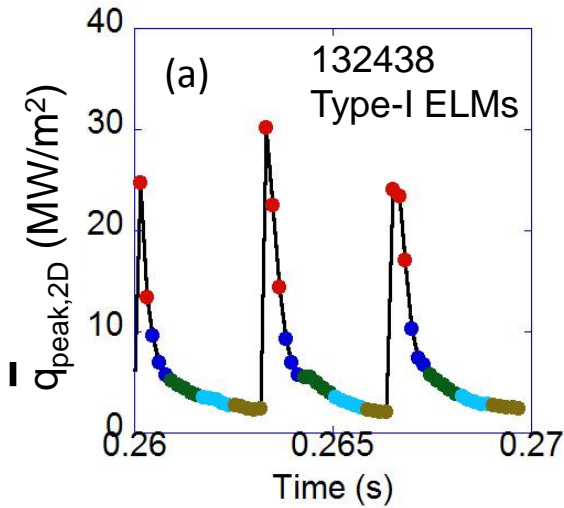


- Type-V ELM is a small ELM regime identified in NSTX<sup>1</sup>
- Heat flux width increases during the ELM, similar to type-III ELMs with low  $\beta_p$
- Both toroidal asymmetries increase during the ELM
- The level of DoA( $q_{\text{peak}}$ ) and DoA( $\lambda_q$ ) is similar, contrary to all other types of ELMs

<sup>1</sup>R. Maingi, Nucl. Fusion 45 (2005) 264



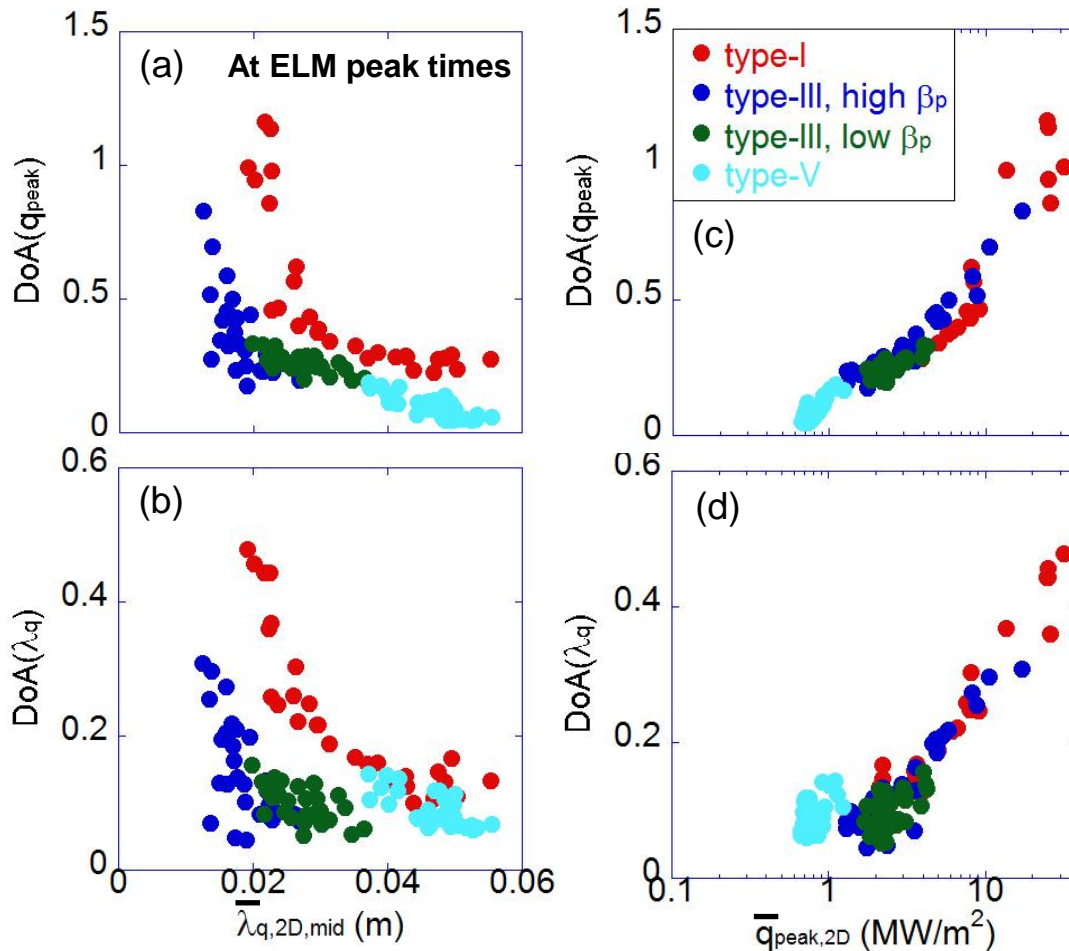
# Behavior of toroidal asymmetries during the ELM cycle for type-I ELMs



- Both  $\text{DoA}(q_{\text{peak}})$  and  $\text{DoA}(\lambda_q)$  become largest at the ELM peak times
- Both DoA values increase with increasing  $q_{\text{peak}}$  and therefore the degree of asymmetric heat deposition is highest at the ELM peak times, while it becomes lower toward the later stage of the inter-ELM period  $\rightarrow$  higher  $q_{\text{peak}}$  leads to higher degree of asymmetric  $q_{\text{peak}}$  and  $\lambda_q$
- The correlation between  $\text{DoA}(q_{\text{peak}})$  and  $\text{DoA}(\lambda_q)$  is the strongest at the ELM peak times and becomes weaker later in the ELM cycle.

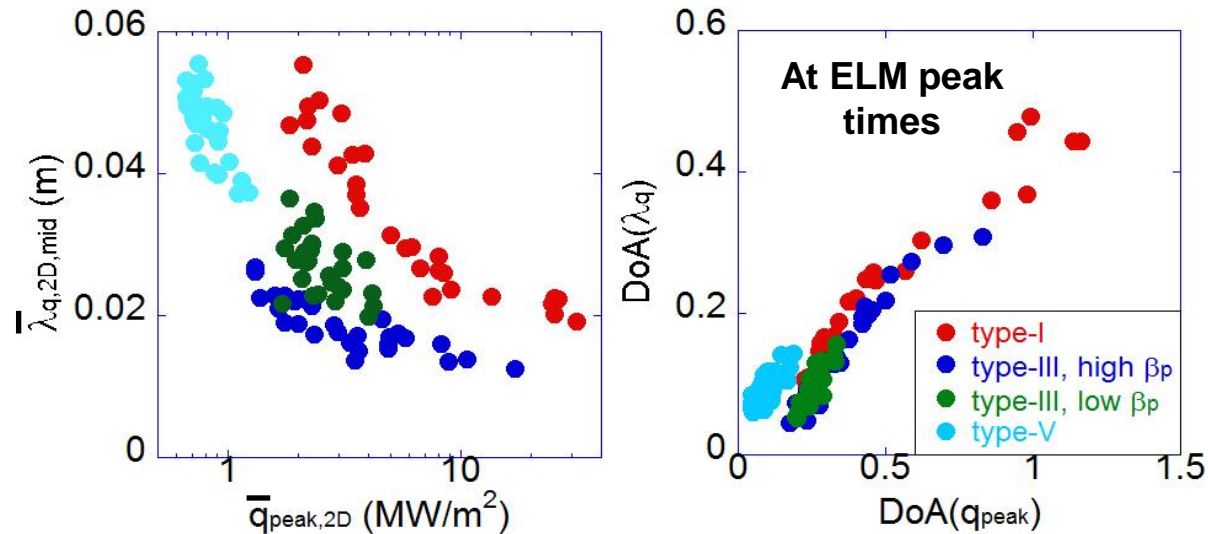


# Dependence of toroidal asymmetries on peak heat flux and mid-plane heat flux width for all ELM types



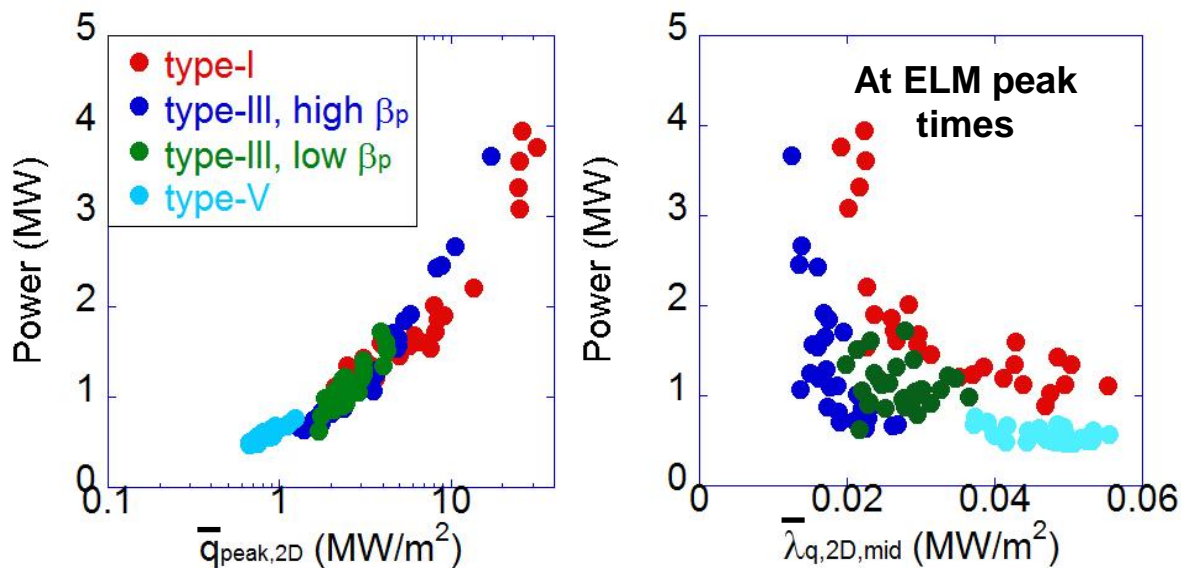
- Comparison of the two DoAs as a function of peak heat flux and heat flux width for all ELM types  $\rightarrow$  Mid-plane heat flux width ( $\bar{\lambda}_{q,2D,\text{mid}}$ ) is used, taking account of the flux expansion
- As a function of  $\bar{\lambda}_{q,2D,\text{mid}}$ : DoAs rapidly decrease with increasing  $\bar{\lambda}_{q,2D,\text{mid}}$  for low  $\bar{\lambda}_{q,2D,\text{mid}}$  ( $\leq 2-2.5$  cm) values, but then the rate of decrease significantly slows down or saturates for  $\bar{\lambda}_{q,2D,\text{mid}} > 2-2.5$  cm.
- As a function of  $\bar{q}_{\text{peak},2D}$ : both DoAs increase with increasing  $q_{\text{peak}}$ , type-V ELMs have relatively higher DoAs

# Correlation between peak heat flux and heat flux width and between the two degrees of asymmetry – all ELM types



- Inverse relationship between heat flux width and peak heat flux is observed generally for all ELM types → not favorable for the extrapolation to the future machine
- Type-V ELMs exhibit the most desired characteristics, *i.e.* the lowest peak heat flux and the largest heat flux width
- The two degrees of asymmetry are found to have positive dependence on each other for all ELM types

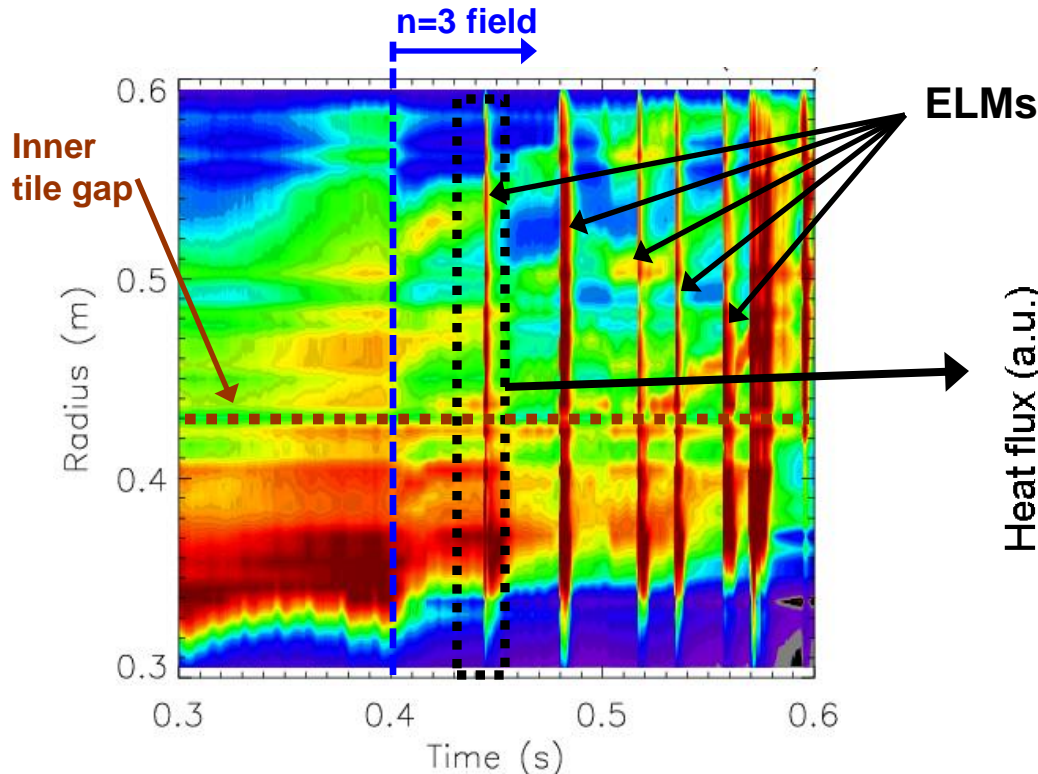
# Dependence of ELM power on peak heat flux and mid-plane heat flux width – all ELM types



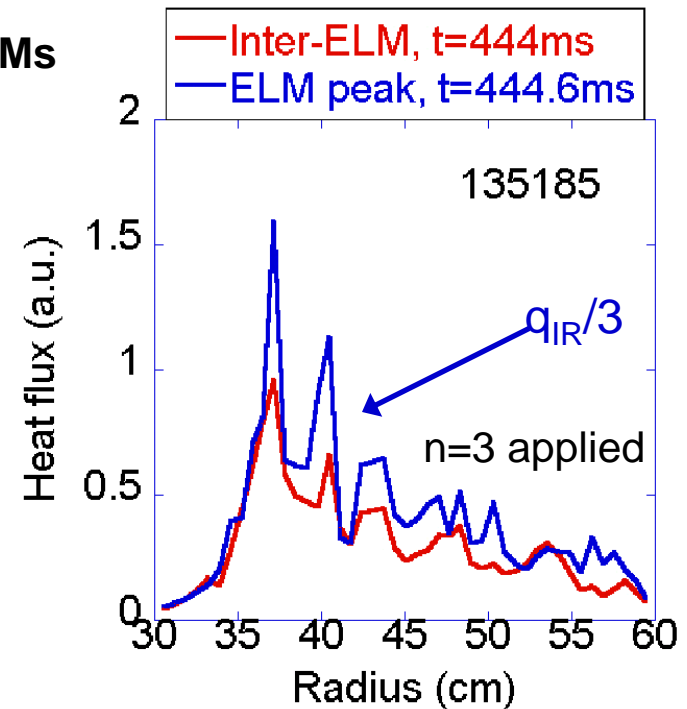
- The total power deposited onto the divertor surface is another important parameter of interest → its dependence on peak heat flux and heat flux width
- The ELM power is a strong function of peak heat flux, forming a consistent trend through all ELM types
- The dependence of power on the mid-plane heat flux width is rather flat for a significant portion of the whole range of heat flux width, except for type-I and high  $\beta_p$  type-III (strong negative dependence at low  $\bar{\lambda}_{q,2D,\text{mid}}$ )

# Heat flux from ELMs triggered by n=3 fields follows imposed field structure

Temporal evolution 1-D heat flux profiles for t = 0.3 – 0.6 sec



1-D heat flux profile for an inter-ELM and at an ELM peak time with 3-D fields applied

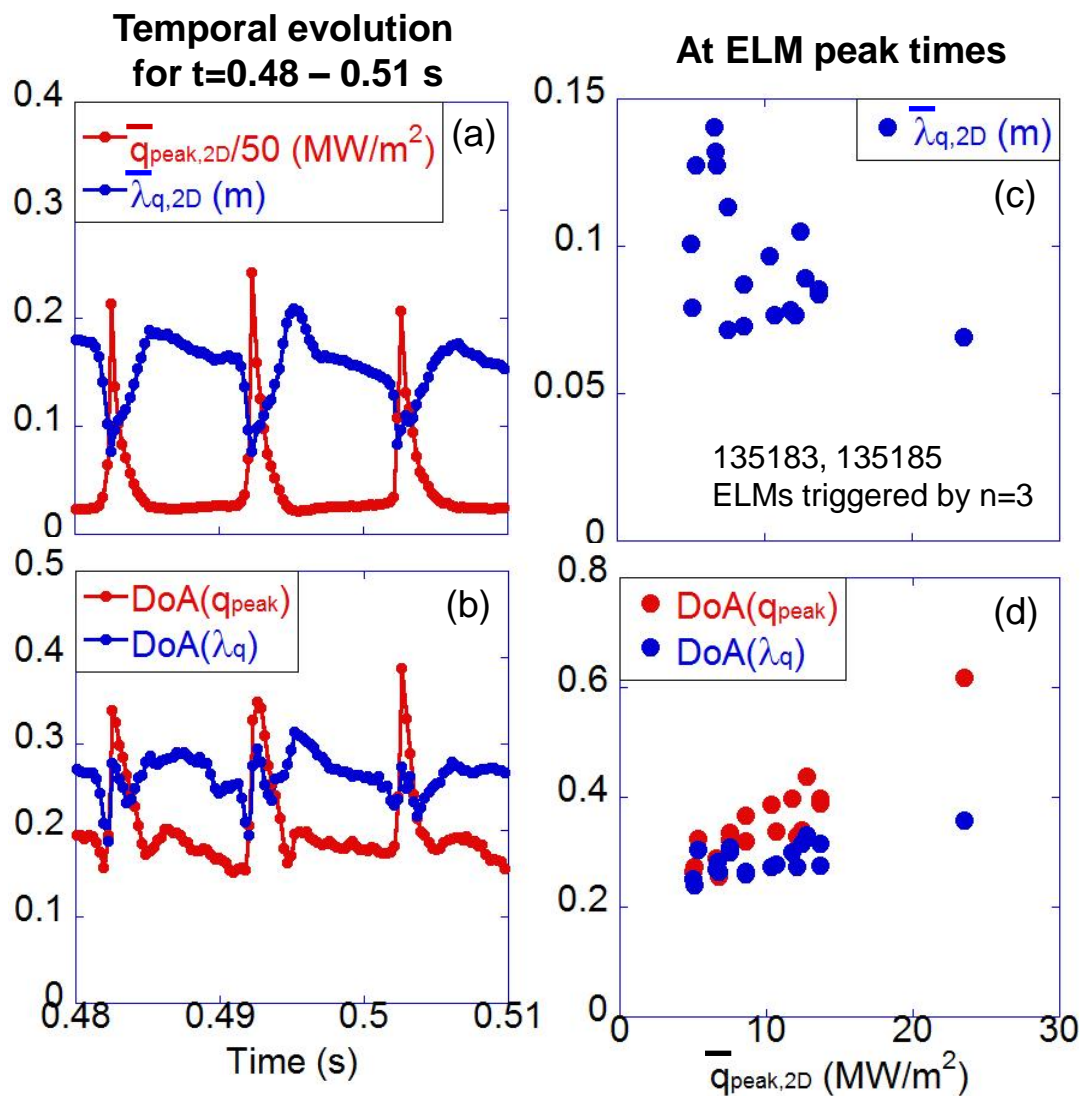


- Striations in the heat flux profile appear in the same locations as before the ELM
- 3-D field (n=3) triggered ELMs in NSTX are phase-locked to the externally applied perturbation structure<sup>1</sup> (also seen in DIII-D<sup>2</sup>)

<sup>1</sup>J-W. Ahn, JNM 415 (2011), S918

<sup>2</sup>M. Jakubowski, NF 49 (2009), 095013

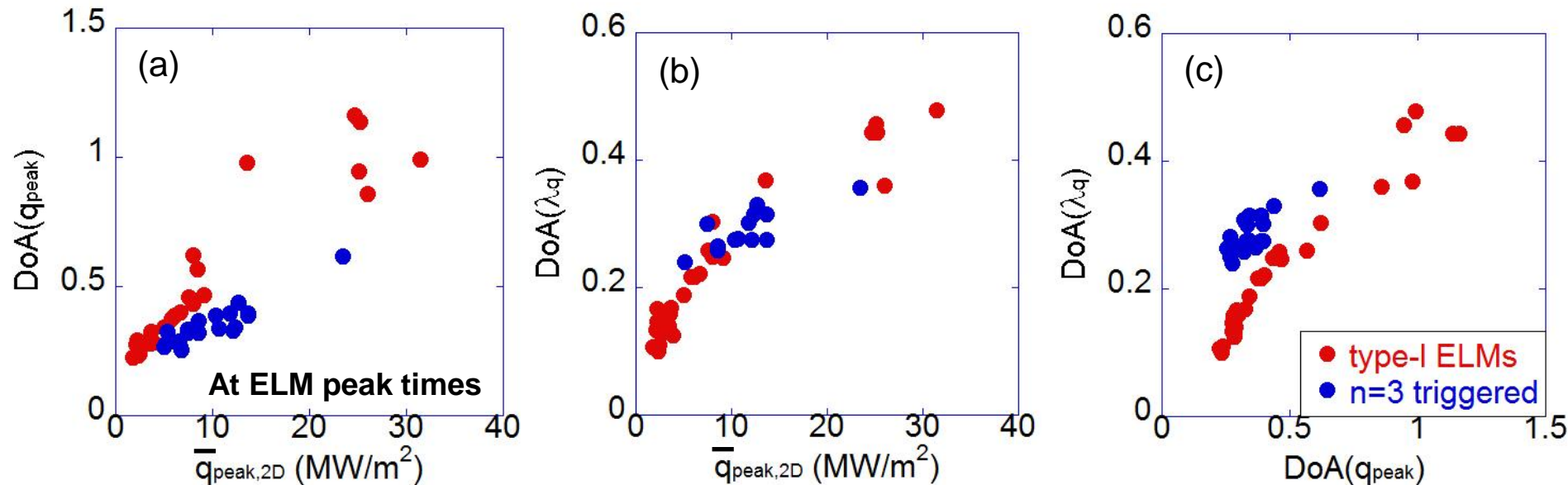
# Behavior of Degree of Asymmetries is not the same as the naturally occurring type-I ELMs – 3-D field triggered ELMs



- Important to examine the characteristics of 2-D heat flux deposition for the triggered ELMs
- The heat flux width drops dramatically by 40-60 % during the ELM
- $\lambda_q$  continues to decrease slowly for a significant fraction of the inter-ELM period → opposite to all types of naturally occurring ELMs
- The increase of  $\text{DoA}(\lambda_q)$  due to the ELM is very weak compared to the inter-ELM level, while  $\text{DoA}(q_{\text{peak}})$  shows a clear spike for each ELM



# Comparison of toroidal asymmetries between naturally occurring type-I ELMs and 3-D field triggered ELMs



- Both for DoA( $q_{\text{peak}}$ ) and DoA( $\lambda_q$ ), the dependence on peak heat flux is noticeably weaker for the triggered ELMs than for the type-I ELMs
- Correlation between DoA( $q_{\text{peak}}$ ) and DoA( $\lambda_q$ ) shows that the variation of DoA( $\lambda_q$ ) is significantly weaker than that of DoA( $q_{\text{peak}}$ )
  - May provide an insight into the mechanism of 3-D field ELM triggering
  - Any relation to the observed phase lock of heat flux profile to the 3-D fields?

# Summary and Conclusions

- Implementation of **TACO** with the incorporation of surface layer effect enables easier study of 2-D heat flux distribution and the toroidal asymmetry of heat flux profiles via remapping of data from  $(x, y)$  to the  $(r, \Phi)$  plane
- The **Degree of Asymmetry (DoA)** was defined for  $q_{\text{peak}}$  and  $\lambda_q$  to quantify how asymmetrically (in the toroidal direction) these two parameters are distributed, as well as the definition of mean value of  $q_{\text{peak}}$  and  $\lambda_q$  for the 2-D plane
- During the ELM,  $\lambda_q$  decreases for type-I and high  $\beta_p$  type-III ELMs but increases for low  $\beta_p$  type-III and type-V ELMs. At ELM peak times,  $\lambda_q$  tends to decrease as  $q_{\text{peak}}$  increases
- Both DoAs, as well as the correlation between the two DoAs, increase with increasing peak heat flux and therefore are highest at the ELM peak times
- $\lambda_{q,\text{mid}}$  variation has no significant impact on DoAs except for low  $\lambda_{q,\text{mid}}$  ( $\sim 2\text{cm}$ )
- Similar level of  $\text{DoA}(q_{\text{peak}})$  and  $\text{DoA}(\lambda_q)$  are observed for **Type-V ELMs**
- **3-D field triggered ELMs have lower level of toroidal asymmetries** compared to naturally occurring type-I ELMs. The range of  $\text{DoA}(\lambda_q)$  is particularly narrower  $\rightarrow$  Any relation to the observed 'phase lock' of heat flux profile to the 3-D fields?